Light-Emitting Paper

*Amir Asadpoordarvish, Andreas Sandström, Christian Larsen, Roger Bollström, Martti Toivakka, Ronald Österbacka, and Ludvig Edman**

A solution-based fabrication of flexible and light-weight light-emitting devices on paper substrates is reported. Two different types of paper substrates are coated with a surface-emitting light-emitting electrochemical cell (LEC) device: a multilayer-coated specialty paper with an intermediate surface roughness of 0.4 µm and a low-end and low-cost copy paper with a large surface roughness of 5 µm. The entire device fabrication is executed using a handheld airbrush, and it is notable that all of the constituent layers are deposited from solution under ambient air. The top-emitting paper-LECs are highly flexible, and display a uniform light emission with a luminance of 200 cd m^{-2} at a current conversion efficacy of 1.4 cd A^{-1}.

1. Introduction

There is currently a tremendous interest, both from academia and industry, in the development and realization of a light-emitting device combining flexibility, light weight, and low cost.[1,2] As it is desirable that this paradigm-shifting emissive device, in addition, should be acceptable from an environmental and safety perspective, and, e.g., be biodegradable and shatter-free upon impact, it is clear that it cannot be fabricated on a conventional glass substrate. A vast majority of the up-to-now executed studies toward this ambitious goal have opted for the fabrication of organic light-emitting diodes (OLEDs) on plastic substrates,[3] although a much lower cost and more environmentally friendly substrate material is available in the form of cellulose-based paper.[2,4] The reason for this choice can be traced to that the performance of the OLED is highly sensitive to that its constituent active-material layers feature exact thicknesses on the nanometer-level,[5] which is a requirement that is difficult to achieve on the rough and porous surface of conventional paper.

Nevertheless, a few publications on the topic of light-emitting devices on paper do exist in the scientific literature. Yoon et al. reported on the fabrication of an OLED on a copy-paper substrate, but the drawbacks from a cost perspective were that the processing included a number of different vacuum steps, with a concomitant limited throughput, and the employment of air-sensitive materials.[6,7] Other reports on OLEDs on paper include the development and employment of a high-end transparent paper,[8] but it is uncertain if such specialty materials ever will develop into becoming true low-cost, i.e., carry a cost of <<€1 m^{-2}. We also note the demonstration of Kim et al. of a high AC-voltage driven electroluminescent device on paper, but the drawback with their fabrication procedure was that it included the poorly scalable employment of a thick spin-on glass smoothing layer.[9] Thus, it is clear that the true vision of a low-cost emissive device on paper has not materialized as of yet.

Here, we report on the solution-based fabrication of light-emitting electrochemical cells (LECs)[10] on two different types of paper substrates: a specialty-paper comprising a multilayer surface coating with a surface roughness of 0.4 µm and a conventional low-cost copy paper with a surface roughness of 5 µm. In the context of the characteristic rough and porous surface of the paper substrates, and the accompanying issue with the necessity for a thick active material, the LEC technology is forgiving because of its electrochemical doping operation that results in the in situ formation of a light-emitting p–n junction doping structure also for mm-thick active materials.[11] The good fit between the LEC operation and the rough paper substrate was demonstrated through the realization of flexible and light-weight top-emitting LEC-on-paper devices, which featured a uniform light emission at a luminance of 200 cd m^{-2} and a current conversion efficacy of 1.4 cd A^{-1}. It is further notable that the entire device fabrication was executed using a handheld airbrush, and that all of the constituent layers were deposited from solution under ambient air.

2. Results and Discussion

Scanning electron microscopy (SEM) images and surface roughness maps recorded on the low-end copy paper and the multilayer-coated specialty paper are displayed in **Figure 1**a–d. The copy-paper, which is available for purchase in regular

A. Asadpoordarvish, Dr. C. Larsen, Prof. L. Edman
The Organic Photonics and Electronics Group
Umeå University
SE-901 87 Umeå, Sweden
E-mail: ludvig.edman@physics.umu.se
A. Asadpoordarvish, Dr. A. Sandström, Dr. C. Larsen, Prof. L. Edman
LunaLEC, Tvistevägen 47, PO Box 7970, SE-907 19 Umeå, Sweden
Dr. R. Bollström, Prof. M. Toivakka, Prof. R. Österbacka
Center for Functional Materials
Åbo Akademi University
FI-20500 Turku, Finland
Dr. R. Bollström
Omya International AG
Baslerstrasse 42, CH-4665, Oftringen, Switzerland

DOI: 10.1002/adfm.201500528

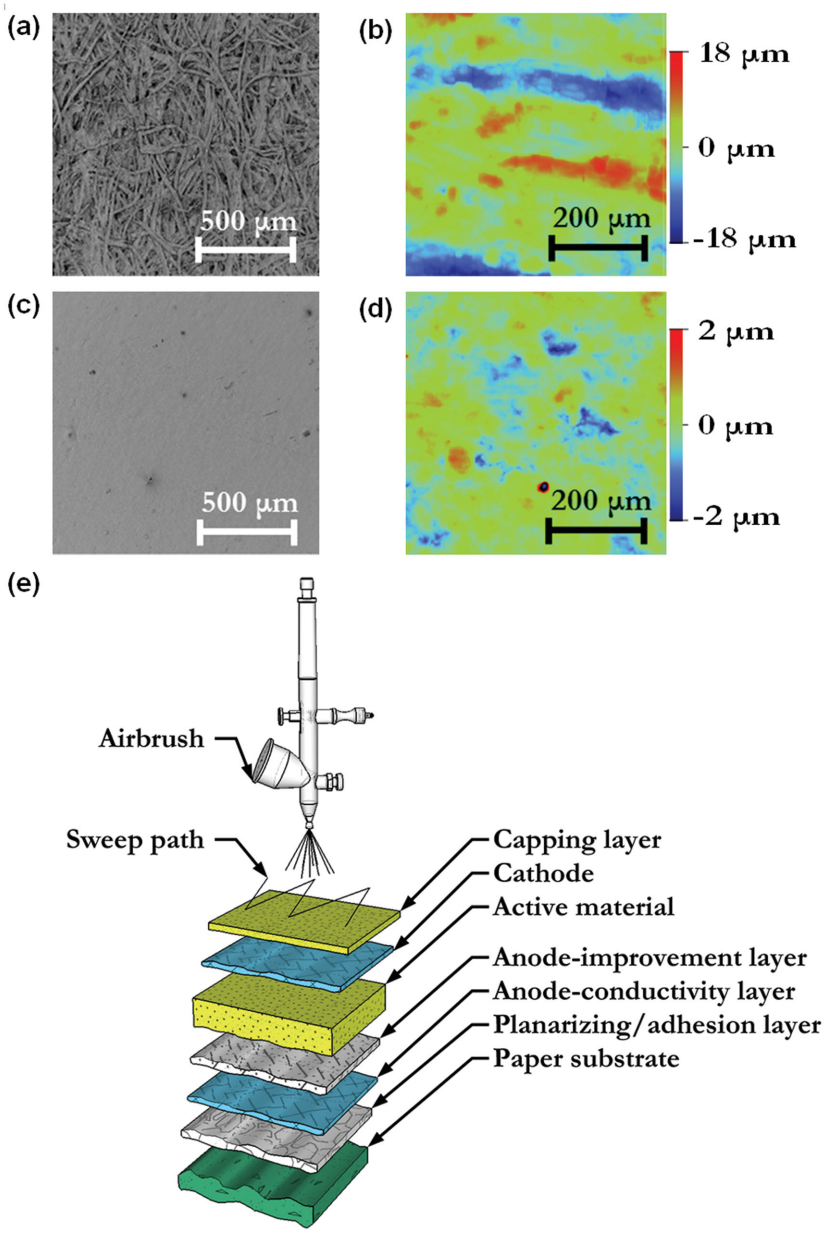

Figure 1. The surface morphology of the copy-paper substrate as characterized with a) SEM and b) surface profilometry, and the surface morphology of the specialty-paper substrate as probed with c) SEM and d) surface profilometry. e) An exploded schematic of the device configuration of the paper-LEC, as fabricated by sequential deposition from solution under ambient air using an airbrush.

convenience stores, features a surface morphology in the form of partially aligned fibrils and a large root-mean-squared (RMS) surface roughness of R_{RMS} = 5.1 μm.

The specialty paper was fabricated by sequential deposition of two different functional layers on a commercial finepaper: i) a 10 g m^{-2} barrier layer consisting of equal parts platy kaolin and ethylene acrylic latex, and ii) a 5 g m^{-2} top coating consisting of 66% fine platy kaolin, 28% fine blocky kaolin and 6% latex. The paper was finally calendered three times through a softnip at a line-load of 120 kN m^{-1} and a temperature of 343 K to improve upon the surface smoothness. Further details on the fabrication of the specialty paper are available in the Experimental Section and in the literature.[12] As expected, the specialty-paper features a flatter surface than the copy-paper, as displayed in Figure 1c,d, and as quantified by a lower R_{RMS} of 0.36 μm.

An exploded-view schematic of the developed functional paper-LEC architecture is shown in Figure 1e. It comprises a bottom trilayer anode, a single-layer active material, and a top cathode; and is an inverted top-emitting device structure as the light generated in the active material will exit the device through the transparent top cathode.[13] It is notable that all of the constituent layers were deposited from solution under ambient air using a handheld airbrush, which is moved over the surface-to-be-coated in a raster-like motion, as depicted schematically in Figure 1e.

The morphology of a spray-deposited film can be controlled through the "wetness" of the spray droplets upon impingement on the surface: If the spray droplets are semidry upon impingement, they can "sinter" together to form a flat-particle-network morphology. Such a spray-sintered film is notably rough, but LEC devices based on a spray-sintered active material have demonstrated an aesthetically appealing homogenous light emission over large areas of hundreds of square centimeters.[14] If the spray droplets instead are wet upon impingement, they will coalesce and form a homogenous wet spray-coated film during coating. The preferred choice of these two manifestations of spray-deposition can be selected through the process parameters, which include solute concentration, solvent vapor pressure, substrate temperature, driving-gas velocity, and nozzle-substrate distance and deposition motion. We opted to keep the last three parameters constant, and thus determined the coated film morphology through the solute concentration, solvent vapor pressure, and substrate temperature. In this work, the anode and cathode layers were selected to be spray-coated while the active material was spray-sintered.

For the copy-paper device, the anode comprised a PEDOT-PSS/Ag-NW/PEDOT-PSS trilayer structure,(PEDOT-PSS is equal to poly(3,4-ethylenedioxythiophene) polystyrene sulfonate and Ag-NW is equal to Ag nanowire) with the purpose of the PEDOT-PSS bottom layer ("the planarizing layer") being to flatten the rough surface of the copy-paper substrate; see Figure S1 in the Supporting Information for an image of the surface morphology of the PEDOT-PSS planarizing layer. For the specialty-paper device, the anode comprised a PEDOT-PSS/Ag-NW/ZnO trilayer structure, where the solution-processed ZnO bottom layer ("the adhesion layer") was included to modify the surface energy of the specialty-paper so that the Ag-NW could adhere more strongly to its surface.[15]

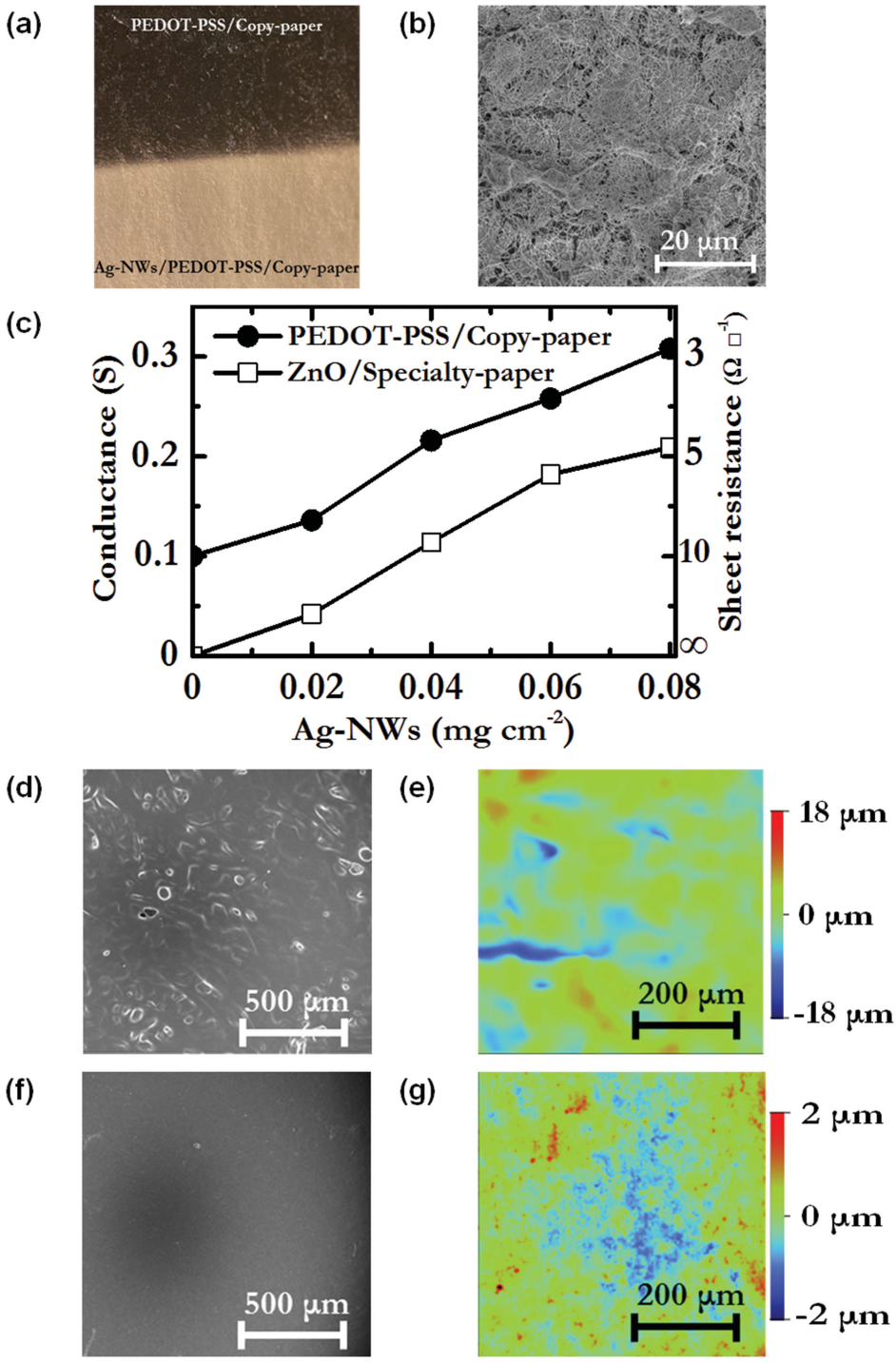

Figure 2. a) Photograph of a PEDOT-PSS/copy-paper substrate, which was spray-coated by Ag-NW only in the lower part, as indicated in the photograph. The addition of the Ag-NW transformed the appearance of the black PEDOT-PSS coating to a reflective surface. b) SEM image of the Ag-NW anode-conductivity layer spray coated (0.08 mg cm^{-2} loading) on the ZnO-coated specialty paper. c) The in situ measured conductance and sheet resistance of the spray-coated anode-conductivity layer as a function of Ag-NW loading, as deposited on the PEDOT-PSS planarization layer on the copy-paper or on the ZnO adhesion layer on the specialty-paper. The anode-coated copy-paper as characterized with d) SEM and e) surface profilometry. The anode-coated specialty-paper as probed with f) SEM and g) surface profilometry.

For both devices, the intermediate Ag-NW layer ("the anode-conductivity layer") was included to provide the required electrode conductivity and to function as a bottom "reflector" so that the generated light could be efficiently coupled out of the device through the transparent top cathode. The latter reflector effect is displayed in the photograph in **Figure 2**a, where the

Ag-NW anode-conductivity layer was selectively deposited on the black PEDOT-PSS coated copy-paper in the lower part of the photograph.

Figure 2c presents the conductance (left) and sheet resistance (right) of the anode-conductivity layer as a function of Ag-NW loading, as measured in situ during the Ag-NW spray coating on substrates positioned on a hot plate kept at 393 K. A schematic of the measurement setup is presented in Figure S2, Supporting Information, and the corresponding data for the PEDOT-PSS planarizing layer are displayed in Table S1, Supporting Information. For the copy-paper device, the sheet resistance and conductivity of the 14.8 µm thick and black PEDOT-PSS planarizing layer were 10 Ω sq^{-1} and 135 S cm^{-1}, respectively; and the Ag-NWs were spray-coated on top of this layer to further decrease the sheet resistance down to 3 Ω sq^{-1} and to provide for a reflective bottom surface. For the specialty-paper, the Ag-NWs were deposited on a 130 nm thin spray-coated ZnO adhesion layer, and a Ag-NW loading of 0.08 mg cm^{-2} resulted in the formation of a reflective film with a low sheet resistance of <5 Ω sq^{-1}.

As the conductance of the layer of high-aspect-ratio Ag-NW is observed to increase in a relatively linear fashion with Ag-NW loading, any potential percolation threshold must be located at a very low Ag-NW concentration. This is also in line with the observed uniform and well-connected network of Ag-NW in the anode-conductivity layer at a loading of 0.08 mg cm^{-2}, as depicted in Figure 2b. This SEM image was recorded on a Ag-NW conductivity layer on the ZnO-coated specialty-paper, but the anode-conductivity layer on the PEDOT-PSS coated copy-paper, as depicted in Figure S3, Supporting Information, appears effectively identical.

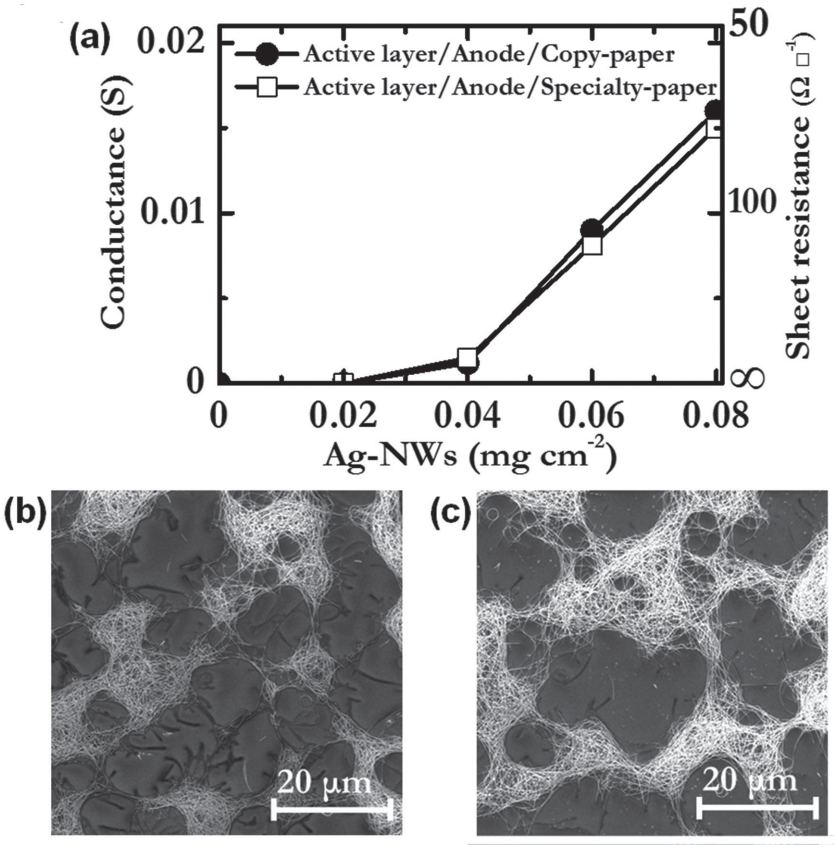

Figure 3. a) The conductance and sheet resistance of the top cathode as a function of Ag-NW loading, as measured in situ during the spray coating of the cathode on the active-material/anode/paper-substrate. SEM images of the Ag-NW cathode (at a loading of 0.08 mg cm^{-2}) as spray-coated on the active-material/anode on top of b) the copy-paper substrate and c) the specialty-paper substrate.

An upper ≈600 nm thin and transparent PEDOT-PSS layer ("the anode-improvement layer") is common to both anode structures, and it was included to planarize the Ag-NW surface so that issues with short circuits through the active layer were suppressed, and to eliminate anodic side reactions by shifting the anodic interface from the Ag-NW to the PEDOT-PSS.[16] SEM images and surface profilometry maps of the complete trilayer anodes as coated on the copy-paper and on the specialty-paper are presented in Figure 2d–g. The aligned-fibril structure of the copy-paper surface (see Figure 1a) is found to be effectively hidden below the anode, and the surface roughness has decreased by 38% to R_{RMS} = 3.2 µm following the anode deposition. The flat surface of the specialty-paper was retained with a comparatively low R_{RMS} of 0.36 µm despite that the anodic fabrication included the deposition of a rough Ag-NW conductivity layer.

The realized anodic surfaces are, however, notably uneven in comparison to conventional flexible ITO-coated plastic substrates, which can feature R_{RMS} values in the sub-10-nm range,[17] i.e., two orders of magnitude lower than the herein fabricated anode-coated paper substrates. Importantly, as the typical flatness requirement for the transport and emissive layers of functional OLEDs is in the same sub-10-nm range,[18] it is not to be expected that the anode-coated paper substrates could be used for the fabrication of OLEDs. LECs can however, in contrast, comprise uneven, and thick, transport and emissive layers and still function satisfactorily.[19] In fact, the transport and emissive functions are commonly combined into one multifunctional active material in an LEC,[20] and Sandström et al. reported that LECs based on a single-layer and highly rough spray-sintered active material film can feature good efficiency and uniform light emission over large areas.[14]

Nevertheless, in order to avoid shorts between the anode and cathode, we elected to spray-sinter a thick layer of active material, being 7.6 µm thick for the copy-paper device and 2.0 µm thick for the specialty-paper device. Figure S4, Supporting Information, shows SEM images of the active material, which comprised a blend of the light-emitting conjugated polymer Super Yellow, the ion transporter PEG-DMA, and the salt KCF_3SO_3 in a 1:0.3:0.03 mass ratio; this particular composition of the active material was selected because we have found it to deliver reasonably good performance in LEC devices with thick active materials.

Figure 3a presents the evolution of the conductance (left) and the sheet resistance (right) of the top Ag-NW cathode,

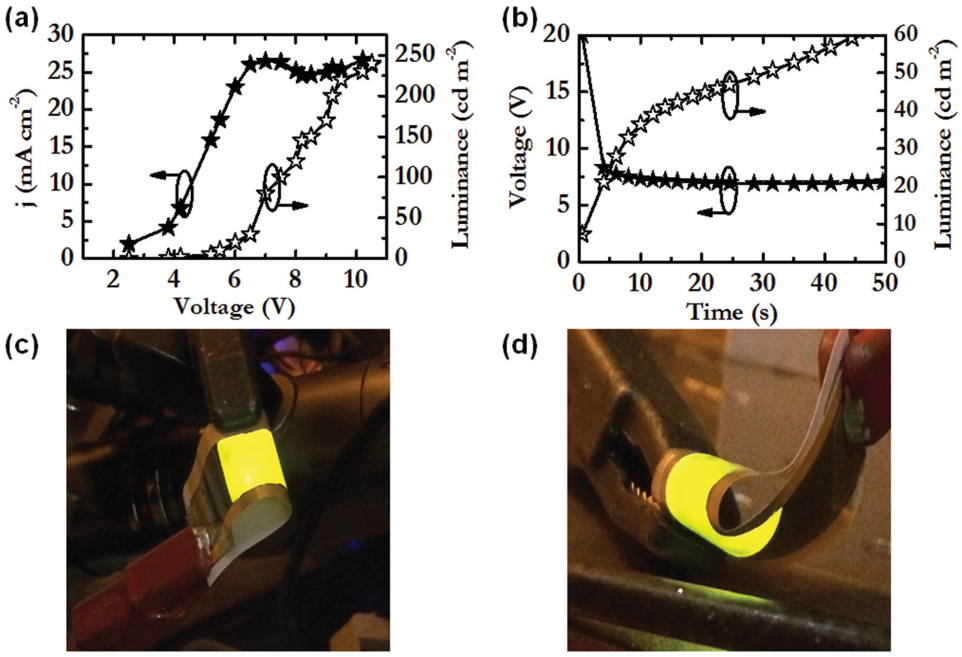

Figure 4. a) The optoelectronic response of a pristine specialty-paper LEC during a voltage ramp of 0.02 V s^{-1}. b) The turn-on process of a specialty-paper LEC during galvanostatic driving at j = 14 mA cm^{-2}. c,d) Photographs of the uniform light emission from bent specialty-paper LECs as driven by j = 5 mA cm^{-2}.

as measured in situ during the spray coating of Ag-NW on top of the active-material/anode/paper-substrate structures maintained at 373 K. We find that the conductance of the cathode features a superlinear dependence on the Ag-NW loading, and that the sheet resistance reaches ≈70 Ω sq^{-1} at a Ag-NW loading of 0.08 mg cm^{-2}, independent of the underlying anode/paper-substrate structure. This value for the sheet resistance is one order of magnitude higher than for the anode-conductivity layer at the same Ag-NW loading; see Figure 2c. SEM images of the Ag-NW cathode in the copy-paper LEC and the specialty-paper LEC are displayed in Figure 3b,c, and they reveal that the Ag-NWs agglomerate into dense regions, which are connected through narrow micrometer-sized Ag-NW bridges. This nonhomogenous morphology of the cathode is distinctly different than the smooth and uniform coating of the anode-conductivity layer (see Figure 2b), and it rationalizes the lower and percolation-type conductivity behavior of the cathode. Moreover, it also explains why the upper cathode layer, as desired, is effectively transparent to the naked eye, whereas the bottom anode-conductivity layer appears reflective. A thin capping layer comprising the active material was finally spray-sintered on top of the cathode in order to keep the Ag-NW in place.

We now shift our attention to the optoelectronic performance of the paper-based LECs, as measured in a N_2-filled glove box. A functional LEC features a number of characteristic properties: i) the device performance is independent on the work function of the electrode materials,[21] ii) the thickness of the active material can be much larger than in an OLED, i.e., >>100 nm,[22] iii) during the initial transient operation at constant-current (galvanostatic) driving, when the active material becomes electrochemically doped and a light-emitting p–n junction is formed in situ, the luminance (L) will increase and the voltage (V) will decrease with time.[23]

Both the copy-paper and the specialty-paper based devices are found to exhibit all of these characteristic features of LEC operation, and **Figure 4**a shows that a pristine specialty-paper LEC displays a low turn-on voltage for the light emission despite the utilization of high work-function Ag-NW and PEDOT-PSS for the cathode and anode, respectively, and the employment of a 2-µm-thick (and rough) active material. The characteristic LEC turn-on process under galvanostatic driving is displayed in Figure 4b for the specialty-paper LEC and in Figure S5, Supporting Information, for the copy-paper LEC. During long-term operation at a current density of j = 14 mA cm^{-2}, the specialty-paper device reached a luminance of 200 cd m^{-2} at a drive voltage of 11 V, which corresponds to a current efficacy (CE) of 1.4 cd A^{-1} and a power conversion efficacy (PCE) of 0.4 lm W^{-1}; see Figure S6, Supporting Information, for data. The copy-paper device driven by j = 3 mA cm^{-2} displayed L = 35 cd m^{-2} at V = 20 V, which corresponds to CE = 1.2 cd A^{-1} and PCE = 0.2 lm W^{-1}. It is notable that the above efficacy values were recorded at maximum luminance. Overall, we find that the distinguishing differences between the specialty-paper LEC and the copy-paper LEC, at this stage of development, are that the specialty-paper LEC features a lower drive voltage and a faster turn-on time (at the same current density), with the former translating into ≈50% higher PCE values for the specialty-paper LECs. We also, quite unexpectedly, find that the voltage is less stable than the luminance during long-term galvanostatic operation for both types of paper-LECs (see Figure S6, Supporting Information).

In order to better evaluate the current potential and shortcomings of the paper-LECs, we have also fabricated and

characterized LECs on glass substrates. These devices comprised a spin-coated film of the same active-material composition, but with a thickness (d) of only 300 nm, as sandwiched between an ITO anode and an Al cathode. The key differences between this "reference" glass-LEC and the paper-LECs are thus that the reference device comprises a much thinner active material (d_{glass} = 300 nm vs $d_{copy\text{-}paper}$ = 7.6 µm and $d_{specialty\text{-}paper}$ = 2 µm), that its electrodes are vacuum-deposited instead of solution-processed, and that it is fabricated on a glass substrate instead of a paper substrate. The typical performance of our pristine glass-LEC is presented in Figure S7, Supporting Information, but we note that a better performance for a similar system has been reported elsewhere.[24] Here, we find that at a drive current density of j = 19.2 mA cm^{-2} results in a luminance of L = 350 cd m^{-2} at V = 3.2 V. This corresponds to efficacy values of: CE = 1.8 cd A^{-1} and PCE = 1.8 lm W^{-1}. Thus, the current efficacy is marginally improved over the paper-LEC, but the main difference is instead to be found in the long-term stability of the drive voltage, which is much better for the glass-LEC. At this stage, we tentatively attribute this shortcoming to a nonadequate cathodic electrochemical stability of the Ag-NW top cathode, and speculate that the inclusion of a ZnO layer in between the active material and the Ag-NW layer could alleviate or eliminate these problems. We also note that the efficiency of the paper-LECs is on par with that reported in ref.[6] for a paper-based OLED.

Nevertheless, the paper-LECs are functional already at this early stage of development, and they do indeed present distinct and important advantages over conventional glass-LEC devices. First, the performance of the paper-LECs was found to be highly tolerant to repeated bending and twisting, and the current-driven 20 mm × 10 mm devices shown in the photographs in Figure 4c,d had been rolled up into a circular shape with a radius of ≈5 mm repeatedly without any observable effect on neither the homogeneity of the light emission, the luminance nor the drive voltage. Thus, the paper-LECs can in contrast to glass-LECs easily be fit and used in nonflat applications, and they also deliver an important safety advantage in that they will not break into (sharp) pieces following impact. Second, the paper-LECs are much lighter than the glass-LECs, due to the fact that the substrate is carrying the majority of the weight in this type of devices. Here, a 20 mm × 10 mm paper-LEC weighed in at 30 mg, whereas the same-sized glass-LEC (on a 1 mm thick glass substrate) weighed 530 mg. Third, the cost of the glass can be very high, and we commonly pay >€100 m^{-2} for our float glass substrates, whereas the cost of, for instance, the copy-paper is very low at €0.1 m^{-2}. However, a main challenge for the practical implementation of the paper-LECs do remain in that a low-cost and high-performance barrier film is lacking; recent work in this field do however suggest that this shortcoming might become resolved in a not-too-distant future.[25]

3. Conclusions

We report on the ambient-air fabrication of functional top-emitting light-emission devices on paper. All of the device layers, including the cathode, active material, and anode, were deposited from solution using a mobile airbrush, and light-emission function was demonstrated on both precoated specialty-paper and low-end copy-paper substrates. A comparison with reference glass-based devices comprising vacuum-deposited electrodes revealed that the solution-processed paper-based devices can compete in terms of efficiency but that the stability of the drive voltage during long-term galvanostatic operation should be further improved. The main merits of the paper-LECs are to be found in the highly flexible form factor, the low-cost substrate and fabrication process, and the low weight.

4. Experimental Section

The copy-paper substrate (thickness = 0.082 mm, "A4 multiuse paper for prints and copies," Staples, USA) was dried in a vacuum oven (p = 1 × 10^{-3} mbar, T = 393 K) for 12 h before use. The specialty-paper (total thickness = 0.083 mm) was produced at the Metso Paper Järvenpää pilot facility (today: Valmet Paper Technology Center) with the slide-curtain coating technique.[12,15] A commercial finepaper (Lumipress 115, StoraEnso, FI) was the basepaper onto which a 10 g m^{-2} barrier layer consisting of platy kaolin (Barrisurf HX, Imerys Minerals Ltd, UK) blended with 50 pph ethylene acrylic latex (Aquaseal 2077, Paramelt B.V., NL) was coated. To adjust printability a 5 g m^{-2} top coating consisting of 70 pph fine platy kaolin (Barrisurf FX, Imerys Minerals Ltd. UK) and 30 pph fine blocky kaolin (Alphatex, Imerys Minerals Ltd., UK) blended with 6 pph styrene-butadiene latex (Basonal 2020.5, BASF, GER) was coated on top of the barrier layer. The paper was calendered three times through a softnip at a lineload of 120 kN m^{-1} and a temperature of 343 K to improve the surface smoothness. The paper substrates were stored in a N_2-filled glovebox ([O_2], [H_2O] < 10 ppm) and cut into 51 mm × 51 mm squares, which were fixed onto glass plates using a piece of tape (width = 6.3 mm, Ted Pella), before use.

The anode comprised three layers with different function, as depicted in Figure 1e. For the planarization layer on the copy-paper, a PEDOT-PSS dispersion (Heraeus, Catalogue Number: Clevios S V3) was diluted with an equal volume of methanol (Sigma-Aldrich). The diluted dispersion was first shaken for 5 min and thereafter sonicated for 60 min. 10 mL of the prepared PEDOT-PSS dispersion was spray-coated onto a masked 50 mm × 50 mm area of the copy-paper substrate kept at 393 K so that a ≈14.8 µm dry black film formed. The spray coating was typically executed in ≈160 back-and-forth sweeps (Figure 1e), with a spray rate of 0.6 mL min^{-1}. The PEDOT-PSS coated copy-paper was dried in the vacuum oven for 12 h. For the adhesion layer on the specialty-paper, 1 mL zinc acetylacetonate hydrate solution ($Zn(acac)_2$, 20 mg mL^{-1} in ethanol, Sigma-Aldrich) was first filtered through a polytetrafluoroethylene filter (pore size: 0.45 µm), then spray-coated onto a masked 50 mm × 50 mm region of the specialty-paper substrate, and finally converted into a 130 nm dry ZnO film by heating at 393 K for ≈5 min. The ZnO conversion process is described in detail in previous work.[26] The spray coating was typically executed in seven back-and-forth sweeps at a 1 mL min^{-1} rate. For the anode-conductivity layer, a Ag-NW dispersion (concentration: 10 mg mL^{-1} in ethanol, wire diameter: 35 nm, wire length: 10 µm, Blue Nano, Catalogue Number: SLV-NW-35) was shaken for 5 min, and then diluted by addition of 19 mL of methanol to 1 mL of ethanol dispersion. The diluted dispersion was sonicated for 15 s, and 4 mL of the prepared Ag-NW dispersion was thereafter spray-coated onto the bottom layer of the anode, as kept at 393 K. The spray coating was typically executed in 20 back-and-forth sweeps with 1.3 mL min^{-1} spraying rate. For the anode-improvement layer, the PEDOT-PSS dispersion (Clevios S V3) was diluted with methanol (Sigma-Aldrich) in a volume ratio of 1:3. The diluted dispersion was shaken for 5 min and sonicated for 60 min. 1 mL of the prepared PEDOT-PSS dispersion was filtered through a glass-fiber filter (pore size: 1 µm) and spray-coated onto the intermediate Ag-NW layer, which was kept at 393 K. The spray coating was typically executed in ten back-and-forth

sweeps at 0.5 mL min^{-1} rate, and resulted in a ≈600 nm thick layer of PEDOT-PSS. The anode-coated substrates were dried in the vacuum oven at $p = 1 \times 10^{-3}$ mbar and $T = 393$ K for 12 h.

The light-emitting conjugated polymer Super Yellow (SY, Merck, Catalogue Number: PDY-132) was dissolved in toluene (Sigma-Aldrich) under vigorous stirring for 12 h at $T = 333$ K. Poly(ethylene glycol)-dimethacrylate (PEG-DMA, Sigma-Aldrich) was dissolved in tetrahydrofuran (Sigma-Aldrich) at room temperature for 3 h. The KCF_3SO_3 salt (Sigma-Aldrich) was dried in the vacuum oven ($p = 1 \times 10^{-3}$ mbar, $T = 393$ K), and dissolved in cyclohexanone (Sigma-Aldrich) at $T = 333$ K for 12 h. The prepared salt solution was filtered through a glass-fiber filter (Sigma-Aldrich, pore size = 1 μm) in order to remove potential particle contaminants. All three master solutions were prepared in a concentration of 10 mg mL^{-1}. The active-layer ink was prepared by blending the master solutions in a mass ratio of {SY:PEG-DMA:KCF_3SO_3} = {1:0.3:0.03}. For the fabrication of copy-paper devices, 10 mL of nondiluted active-layer ink was spray-sintered onto the anode-coated substrate kept at 373 K, during ≈65 back-and-forth sweeps at a rate of 1.1 mL min^{-1}. For the specialty-paper devices, 3 mL active-layer ink was diluted by addition of 7.5 mL toluene and 1.25 mL cyclohexanone. The diluted active-layer ink was shaken vigorously and stored for 15 min before deposition. 7 mL of diluted ink was thereafter spray-sintered onto the anode-coated substrates kept at 373 K, during 18 back-and-forth sweeps at a rate of 2.6 mL min^{-1}. The dry thickness of the active layer was 7.6 μm (for the copy-paper device) and 2 μm (for the specialty-paper device).

The cathode was fabricated by first spray coating the Ag-NW dispersion on top of the active layer in accordance with the procedure detailed for the anode-conductivity layer above. Thereafter, 1.5 mL of the diluted active-layer ink was sprayed on top of the Ag-NW film kept at 373 K to form a "capping layer," which kept the Ag-NWs in place. The complete LEC device was finally dried in the vacuum oven ($T = 343$ K, $p = 1 \times 10^{-3}$ mbar) for 24 h. The anode, active layer, and cathode were all spray-deposited using a handheld airbrush (Biltema, Catalogue Number: 17–362), with the driving N_2-gas pressure and the nozzle-substrate distance kept constant at $p = 3$ bar and 10 cm, respectively, throughout all experiments. It is notable that all constituent materials were dissolved and processed under ambient air. In order to alleviate issues with clogging of the airbrush nozzle, we opted to dilute and/or filter thick inks with high viscosity, as detailed above. The thickness and surface morphology of the deposited layers were measured with a stylus profilometer (Dektak XT, Bruker). The SEM images were recorded with a field-emission SEM (Zeiss Merlin, GmbH) using a secondary electron detector, a beam accelerating voltage of 4 kV, and a probe current of 150 pA. The samples were cut into small pieces and mounted onto Al stubs using carbon adhesive tape. For nonconductive surfaces a ≈5 nm thin layer of Au or Au/Pd was deposited on the surface before probing. The conductance of the electrode materials was measured with a two-electrode setup using Ag contact pads (area: 5 mm × 50 mm, thickness: 100 nm), which were thermally evaporated on two opposing sides of a paper at a distance of 50 mm from each other, as shown schematically in Figure S2 in the Supporting Information. All presented data were measured on at least two independent films, and the variation in conductance was found to be negligible. The LEC devices were characterized using a computer-controlled source-measure unit (Keithley 2400) and a calibrated photodiode, equipped with an eye-response filter (Hamamatsu Photonics, S9219–01), connected to a data GPIB controller (National Instruments, GPIB-USB-HS) via a current-to-voltage amplifier. The accuracy of the luminance data were verified with a luminance meter (Konica Minolta, LS-110).

Supporting Information

Supporting Information is available from the Wiley Online Library or from the author.

Acknowledgements

A.A., C.L., and L.E. acknowledge the Swedish Foundation for Strategic Research, Vetenskapsrådet, Energimyndigheten, Kempestiftelserna, and Umeå University for financial support. L.E. is a Royal Swedish Academy of Sciences Research Fellow supported by a grant from the Knut and Alice Wallenberg Foundation. The authors also acknowledge the Umeå Core Facility Electron Microscopy (UCEM) at the Chemical Biological Centre (KBC), Umeå University, for use of facilities and technical assistance.

Received: February 7, 2015
Revised: March 26, 2015
Published online: April 15, 2015

[1] *Flexible OLED Reports*, Vol. *2014*, UBI research, www.ubiresearch.com/2014-flexible-oled-report/, Seoul, Korea, **2014**.
[2] D. Graham-Rowe, *Nat. Photon* **2007**, *1*, 248.
[3] a) L. Zhou, H.-Y. Xiang, S. Shen, Y.-Q. Li, J.-D. Chen, H.-J. Xie, I. A. Goldthorpe, L.-S. Chen, S.-T. Lee, J.-X. Tang, *ACS Nano* **2014**, *8*, 12796; b) T.-B. Song, N. Li, *Electronics* **2014**, *3*, 190.
[4] a) R. Osterbacka, J.-W. Han, *Nanotechnology* **2014**, *25*, 090201; b) M. Irimia-Vladu, E. D. Głowacki, G. Voss, S. Bauer, N. S. Sariciftci, *Mater. Today* **2012**, *15*, 340; c) D. Tobjork, R. Osterbacka, *Adv. Mater.* **2011**, *23*, 1935.
[5] a) J. W. Park, T. W. Kim, J. B. Park, *Semicond. Sci. Technol.* **2013**, *28*, 045013; b) A. Perumal, H. Faber, N. Yaacobi-Gross, P. Pattanasattayavong, C. Burgess, S. Jha, M. A. McLachlan, P. N. Stavrinou, T. D. Anthopoulos, D. D. C. Bradley, *Adv. Mater.* **2015**, *27*, 93; c) S. Hofle, A. Schienle, C. Bernhard, M. Bruns, U. Lemmer, A. Colsmann, *Adv. Mater.* **2014**, *26*, 5155.
[6] D.-Y. Yoon, D.-G. Moon, *Curr. Appl. Phys.* **2012**, *12*, e29.
[7] D. Y. Yoon, T. Y. Kim, D. G. Moon, *Curr. Appl. Phys.* **2010**, *10*, E135.
[8] a) J. H. Song, R. J. Murphy, R. Narayan, G. B. H. Davies, *Philos. Trans. R. Soc., B* **2009**, *364*, 2127; b)S. Purandare, E. F. Gomez, A. J. Steckl, *Nanotechnology* **2014**, *25*, 094012; c) C. Legnani, C. Vilani, V. L. Calil, H. S. Barud, W. G. Quirino, C. A. Achete, S. J. L. Ribeiro, M. Cremona, *Thin Solid Films* **2008**, *517*, 1016; d) M. Nogi, H. Yano, *Adv. Mater.* **2008**, *20*, 1849.
[9] J. Y. Kim, S. H. Park, T. Jeong, M. J. Bae, S. Song, J. Lee, I. T. Han, D. Jung, S. Yu, *IEEE Trans. Electron Devices* **2010**, *57*, 1470.
[10] a) S. B. Meier, D. Tordera, A. Pertegas, C. Roldan-Carmona, E. Orti, H. J. Bolink, *Mater. Today* **2014**, *17*, 217; b) Q. B. Pei, G. Yu, C. Zhang, Y. Yang, A. J. Heeger, *Science* **1995**, *269*, 1086; c) J. M. Leger, *Adv. Mater.* **2008**, *20*, 837; d) S. Tang, J. Y. Pan, H. A. Buchholz, L. Edman, *J. Am. Chem. Soc.* **2013**, *135*, 3647; e) H. C. Su, C. Y. Cheng, *Isr. J. Chem.* **2014**, *54*, 855.
[11] a) P. Matyba, K. Maturova, M. Kemerink, N. D. Robinson, L. Edman, *Nat. Mater.* **2009**, *8*, 672; b) J. Gao, J. Dane, *Appl. Phys. Lett.* **2003**, *83*, 3027; c) Y. Hu, J. Gao, *J. Am. Chem. Soc.* **2011**, *133*, 2227; d) P. Matyba, M. R. Andersson, L. Edman, *Org. Electron.* **2008**, *9*, 699; e) G. Gozzi, L. D. Cagnani, R. M. Faria, L. F. Santos, *J.Solid State Electrochem.* **2014**, *18*, 3181; f) J. Liu, I. Engquist, M. Berggren, *J. Am. Chem. Soc.* **2013**, *135*, 12224.
[12] a) R. Bollstrom, F. Pettersson, P. Dolietis, J. Preston, R. Osterbacka, M. Toivakka, *Nanotechnology* **2014**, *25*, 094003; b) R. Bollstrom, D. Tobjork, P. Dolietis, P. Salminen, J. Preston, R. Osterbacka, M. Toivakka, *Chem. Eng. Process.* **2013**, *68*, 13.
[13] W. R. Cao, J. Li, H. Z. Chen, J. G. Xue, *J. Photonics Energy* **2014**, *4*, 040990.
[14] A. Sandström, A. Asadpoordarvish, J. Enevold, L. Edman, *Adv. Mater.* **2014**, *26*, 4975.
[15] R. Bollström, A. Määttänen, D. Tobjörk, P. Ihalainen, N. Kaihovirta, R. Österbacka, J. Peltonen, M. Toivakka, *Org. Electron.* **2009**, *10*, 1020.

[16] J. H. Shin, P. Matyba, N. D. Robinson, L. Edman, *Electrochim. Acta* **2007**, *52*, 6456.
[17] Y. Yang, Q. Huang, A. W. Metz, J. Ni, S. Jin, T. J. Marks, M. E. Madsen, A. DiVenere, S. T. Ho, *Adv. Mater.* **2004**, *16*, 321.
[18] C. Jonda, A. B. R. Mayer, U. Stolz, A. Elschner, A. Karbach, *J. Mater. Sci.* **2000**, *35*, 5645.
[19] S. Tang, A. Sandstrom, J. F. Fang, L. Edman, *J. Am. Chem. Soc.* **2012**, *134*, 14050.
[20] A. Sandstrom, H. F. Dam, F. C. Krebs, L. Edman, *Nat. Commun.* **2012**, *3*, 1002.
[21] a) G. Hernandez-Sosa, R. Eckstein, S. Tekoglu, T. Becker, F. Mathies, U. Lemmer, N. Mechau, *Org. Electron.* **2013**, *14*, 2223; b)G. Hernandez-Sosa, S. Tekoglu, S. Stolz, R. Eckstein, C. Teusch, J. Trapp, U. Lemmer, M. Hamburger, N. Mechau, *Adv. Mater.* **2014**, *26*, 3235–3240; c) J. J. Liang, L. Li, X. F. Niu, Z. B. Yu, Q. B. Pei, *J. Phys. Chem. C* **2013**, *117*, 16632; d) P. Matyba, H. Yamaguchi, G. Eda, M. Chhowalla, L. Edman, N. D. Robinson, *ACS Nano* **2010**, *4*, 637.
[22] X. Y. Li, J. Gao, G. J. Liu, *Org. Electron.* **2013**, *14*, 1441.
[23] a) S. van Reenen, P. Matyba, A. Dzwilewski, R. A. J. Janssen, L. Edman, M. Kemerink, *J. Am. Chem. Soc.* **2010**, *132*, 13776; b) S. van Reenen, T. Akatsuka, D. Tordera, M. Kemerink, H. J. Bolink, *J. Am. Chem. Soc.* **2013**, *135*, 886.
[24] Z. Yu, M. Wang, G. Lei, J. Liu, L. Li, Q. Pei, *J. Chem. Phys. Lett.* **2011**, *2*, 367.
[25] H. Yamaguchi, J. Granstrom, W. Nie, H. Sojoudi, T. Fujita, D. Voiry, M. Chen, G. Gupta, A. D. Mohite, S. Graham, M. Chhowalla, *Adv. Energy Mater.* **2014**, *4*, 1300986.
[26] P. de Bruyn, D. J. D. Moet, P. W. M. Blom, *Org. Electron.* **2010**, *11*, 1419.